ARTICLE NO. 79-4150

Examination of the Flap-Lag Stability of Rigid Articulated Rotor Blades

K. R. V. Kaza*
NASA Lewis Research Center, Cleveland, Ohio
and
R. G. Kvaternik†
NASA Langley Research Center, Hampton, Va.

A critical examination of flap-lag stability of a centrally hinged, spring-restrained rigid blade in both hover and forward flight is presented. Several differences in the equations of motion for blade flap-lag stability in the existing literature are identified. A rigorous and systematic development of these equations for a rigid articulated blade in forward flight shows the existence of some linear aerodynamic coupling terms associated with blade steady-state flapping and lagging in the perturbation equations. The differences identified are shown to be associated with whether or not the lag hinge flaps with the blade. The implications of these differences on stability are examined, and it is shown that the pitch-lag coupling terms associated with a hinge arrangement in which the lag hinge flaps with the blade have a marked influence on flap-lag stability, depending on the system parameters.

Nomenclature

a	= section lift curve slope
b	= number of blades
c	= section chord
C_{d_0}	= blade mean profile drag coefficient
c_β, c_ζ	= viscous damping coefficient in flap and lag, respectively
C_T	= thrust coefficient
C_H	= horizontal force coefficient
$\mathrm{d}L, \mathrm{d}D$	= incremental lift and drag forces, respectively
D_P	= parasite drag
$\hat{e}_x, \hat{e}_y, \ldots, \hat{e}_{z_2}$	= unit vectors
$\mathrm{d}F_x, \mathrm{d}F_y, \ldots, \mathrm{d}F_{z_2}$	= components of elemental forces
H	= rotor longitudinal force
I	= mass moment of inertia of blade in flap and lag
k_β, k_ζ	= spring rate about flap and lag hinges, respectively
M_β, M_ζ	= aerodynamic moments in flap and lag, respectively
p	= dimensionless rotating flapping natural frequency at $\theta=0$
r	= spanwise position of blade element
R	= blade tip radius
T	= rotor thrust; kinetic energy
U	= resultant velocity perpendicular to blade-span axis at blade element
U_R, U_P, U_T	= relative radial, normal, and tangential velocity components
V	= magnitude of forward flight velocity; potential energy
V_a	= wind velocity vector [Eq. (16)]
V_{xyz}	= total velocity vector [Eq. (17)]
v_i	= induced velocity at rotor, positive downward
X, Y, Z	= inertial axes in hub plane with origin at hub
xyz	= hub-fixed rotating axes
$x_2y_2z_2$	= blade-fixed rotating axes
Y	= rotor side force
α	= blade section angle of attack; angle between shaft axis and plane perpendicular to flight path, positive when axis is pointing rearward
β	= flapping angular displacement of blade measured from plane of rotation, positive upward
γ	= blade Lock number, $\gamma=\rho acR^4/I$
ζ	= lead-lag angular displacement of blade, positive in direction of rotor rotation
ζ_β, ζ_ζ	= viscous damping ratio in flap and lag, respectively
θ	= blade section pitch angle, positive leading edge upward
θ_c	= blade collective pitch
θ_{ls}, θ_{lc}	= cyclic pitch components
λ	= inflow ratio $(V\sin\alpha - v_i)/\Omega R$, positive up
μ	= advance ratio, $V\cos\alpha/\Omega R$
ρ	= air mass density
$\boldsymbol{\rho}$	= position vector of blade mass element with respect to hub-fixed rotating axes
σ	= rotor solidity
ϕ	= inflow angle at blade element in plane perpendicular to blade span axis
ψ	= blade azimuth angle measured from downwind position in direction of rotation
Ω	= rotor angular velocity
ω	= angular velocity of hub-fixed rotating axes
$\bar{\nu}_\beta, \bar{\omega}_\zeta$	= nondimensional nonrotating flap and lag natural frequencies, respectively, at $\theta=0$
$(\ )_0, \Delta(\ )$	= steady-state and perturbation variables, respectively
$(\dot{\ })$	= time derivative, $\mathrm{d}(\ )/\mathrm{d}t$
$(\ )^T$	= transpose

Received Sept. 28, 1976; revision received July 23, 1979. This paper is declared a work of the U.S. Government and therefore is in the public domain. Reprints of this article may be ordered from AIAA Special Publications, 1290 Avenue of the Americas, New York, N. Y. 10019. Order by Article No. at top of page. Member price $2.00 each, nonmember, $3.00 each. **Remittance must accompany order.**

This article is based on a portion of Ref. 1 to which new material has been added.

Index categories: Helicopters; Propeller and Rotor Systems; Aeroelasticity and Hydroelasticity.

*Adjunct Associate Professor, Mechanical Engineering Department, University of Toledo, Toledo, Ohio. Member AIAA.

†Aerospace Engineer, Rotorcraft Aeroelasticity Group, Structures and Dynamics Division. Member AIAA.

Introduction

THE analytical efforts directed to blade flap-lag stability which are described in the literature are based on essentially two types of mathematical models. The first model[2-12] consists of a centrally or offset-hinged, spring-restrained rigid blade. This model has been used to analyze rigid articulated blades and hingeless blades approximated by virtual hinges. The second model[13-19] treats the blade as an elastic beam and has been applied to the analysis of hingeless blades. Adopting the first model, the present authors have become involved in some analytical studies related to the flap-lag dynamics of helicopter rotor blades. As part of this effort, the second-degree nonlinear equations of motion for the flap-lag stability of an articulated, centrally hinged, spring-restrained rigid blade were developed. To verify the validity of these equations, comparisons were made with several sets of equations already existing in the literature. These comparisons identified some differences in the aerodynamic terms. The differences which were identified are in some aerodynamic pitch-lag and pitch-flap coupling terms associated with blade steady-state flapping and lagging in the linear perturbation equations. Careful comparative examinations revealed that the differences are a consequence of the arrangement of the flapping and lagging hinges; in particular, whether or not the lag hinge flaps with the blade. In the usual derivation of the equations of motion, the hinge arrangement is reflected in the order in which the flapping and lagging rotational transformations are imposed. In Refs. 2-15 equations of motion have been derived either for the case in which the lag hinge flaps with blade (a flap-lag hinge sequence) or for the case in which the flap hinge lags with the blade (a lag-flap hinge sequence), but not for both, and the effect of hinge sequence on stability has not been addressed. The effect of hinge sequence on flap-lag stability of a rigid articulated blade was identified in Ref. 16 for the case of hover. These results and the accompanying discussion are, however, unclear with regard to the differences in the equations of motion which are associated with the hinge sequence and the role of the hinge sequence in flap-lag stability.

The purpose of this paper is to explain these differences by deriving in detail the flap-lag equations of motion of a rigid blade in forward flight assuming both flap-lag and lag-flap hinge sequences and to examine the implications of these differences on blade flap-lag stability in both hover and forward flight.

Some Qualitative Considerations

The establishment of the blade flap-lag equations of motion by either energy or Newtonian approaches requires the specification of the position vector of an arbitrary point on the blade in the displaced configuration. This position vector can be conveniently obtained by performing a sequence of rotations and translations from inertial axes fixed in the hub to axes fixed at the arbitrary point on the blade. In such an approach, rotation of coordinate axes corresponds to matrix multiplication and a translation of coordinate axes corresponds to matrix addition. The order of the rotational transformations due to flapping and lagging motions of the blade is of concern here because of the nonlinear nature of the governing equations of motion. It is well recognized that if one is developing a linear set of governing equations, the order in which the transformations are carried out is unimportant. However, if one is developing the second-degree nonlinear equations, care must be taken to insure the retention of all second-degree terms in the product of the transformation matrices. In this case, the transformation matrices associated with rotations are not commutative, and it is quite natural to expect differences in the equations.

Consider the case of the articulated blade shown in Fig. 1. When the flap and lag hinges are noncoincident, the radial

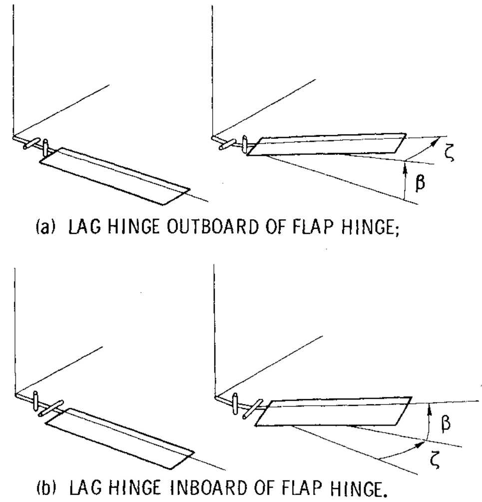

Fig. 1 Hinge geometry for articulated blade.

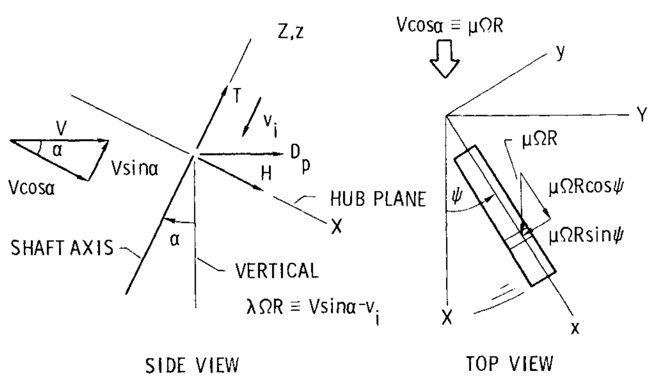

Fig. 2 Geometry for aerodynamic velocity components and for trim calculations.

position of the hinges clearly defines the kinematics of the blade motion and suggests the natural order in which to impose the flapping and lagging rotations to write the position vector of an arbitrary point on the blade. When the flap hinge is inboard of the lag hinge so that the lag hinge flaps with the blade (Fig. 1a), usual practice is to impose a flapping rotation followed by a lagging rotation. When the lag hinge is inboard and does not flap with the blade (Fig. 1b), the rotational transformation sequence is usually lag followed by flap. Now the hinges can also be coincident, in which case the question as to whether or not the lag hinge flaps with the blade must still be addressed since, depending on the structural configuration, it is physically possible to have either situation when the hinges are coincident.

The case of coincident hinges located at the shaft is a simplification often addressed analytically in the literature. However, often it is not clear as to what hinge sequence is being considered. On the basis of the above considerations, for the case of either coincident or noncoincident hinges, if the lag hinge (either physical or virtual) flaps with the blade, the usual transformation sequence while deriving the equations of motion is flap followed by lag, and if the flap hinge lags with the blade, the usual transformation sequence is lag followed by flap. It should be noted that typical hingeless rotor blades have a flap-lag virtual hinge sequence.

Analytical Formulation

In this section, the flap-lag equations of motion for a rigid, articulated blade in forward flight are developed assuming both a flap-lag hinge sequence and a lag-flap hinge sequence. For convenience, the hinges are assumed to be coincident and located at the shaft. The equations are derived in a coordinate system xyz rotating with the hub (Fig. 2). The aerodynamic forces are based on linear, quasisteady strip theory; stall, compressibility, and reversed flow are not considered. The induced inflow is assumed to be uniform and is obtained from momentum theory.

Dynamics

For a flap-lag hinge sequence, the usual rotational transformation sequence is flap followed by lag. For this case, the hub-fixed rotating axes xyz are related to the blade-fixed axes $x_2y_2z_2$ according to

$$\begin{Bmatrix} x \\ y \\ z \end{Bmatrix} = [T_{\rm FL}] \begin{Bmatrix} x_2 \\ y_2 \\ z_2 \end{Bmatrix} \tag{1}$$

where

$$[T_{\rm FL}] = [T_\beta][T_\zeta] \tag{2}$$

$$= \begin{bmatrix} \cos\beta & 0 & -\sin\beta \\ 0 & 1 & 0 \\ \sin\beta & 0 & \cos\beta \end{bmatrix} \begin{bmatrix} \cos\zeta & -\sin\zeta & 0 \\ \sin\zeta & \cos\zeta & 0 \\ 0 & 0 & 1 \end{bmatrix} \tag{3}$$

Using Eq. (1), the position vector of an arbitrary mass point on the elastic axis of the blade ($x_2 = r, y_2 = z_2 = 0$) is given by

$$\rho = r\cos\beta\cos\zeta\hat{e}_x + r\sin\zeta\hat{e}_y + r\sin\beta\cos\zeta\hat{e}_z \tag{4}$$

Noting that the angular velocity of the xyz system with respect to inertial axes can be written as

$$\omega = \Omega\hat{e}_z \tag{5}$$

the absolute velocity of the mass point expressed in the hub-fixed rotating system xyz is

$$\dot{\rho} \equiv \frac{d\rho}{dt} = \frac{\partial\rho}{\partial t} + \omega\times\rho \tag{6}$$

which leads to

$$\begin{aligned}\dot{\rho} = & -r(\cos\beta\sin\zeta\dot{\zeta} + \cos\zeta\sin\beta\dot{\beta} \\ & + \Omega\sin\zeta)\hat{e}_x + r(\cos\zeta\dot{\zeta} + \Omega\cos\beta\cos\zeta)\hat{e}_y \\ & + r(\cos\zeta\cos\beta\dot{\beta} - \sin\beta\sin\zeta\dot{\zeta})\hat{e}_z \end{aligned} \tag{7}$$

Substituting $\dot{\rho}$ into the kinetic energy expression

$$T = \tfrac{1}{2}\int_0^R (\dot{\rho}\cdot\dot{\rho})dm \tag{8}$$

leads to

$$\begin{aligned} T = & \tfrac{1}{2}I[\dot{\zeta}^2 + \dot{\beta}^2\cos^2\zeta + \Omega^2(\sin^2\zeta + \cos^2\zeta\cos^2\beta) \\ & + 2\Omega\dot{\beta}\sin\beta\sin\zeta\cos\zeta + 2\Omega\dot{\zeta}\cos\beta] \end{aligned} \tag{9}$$

where the blade flapping and lagging inertias, assumed to be equal, are given by

$$I = \int_0^R r^2 dm \tag{10}$$

The potential energy and dissipation functions are

$$V = \tfrac{1}{2}k_\beta\beta^2 + \tfrac{1}{2}k_\zeta\zeta^2 \tag{11}$$

$$D = \tfrac{1}{2}c_\beta\dot{\beta}^2 + \tfrac{1}{2}c_\zeta\dot{\zeta}^2 \tag{12}$$

Substituting Eqs. (9), (11), and (12) into Lagrange's equation and retaining terms through second degree in the dependent variables β and ζ leads to

$$\ddot{\beta} + 2\Omega\dot{\zeta}\beta + 2\zeta_\beta p\Omega\dot{\beta} + p^2\Omega^2\beta = M_\beta/I \tag{13a}$$

$$\ddot{\zeta} + 2\Omega\beta\dot{\beta} + 2\zeta_\zeta\bar{\omega}_\zeta\Omega\dot{\zeta} + \Omega^2\bar{\omega}_\zeta^2\zeta = M_\zeta/I \tag{13b}$$

where M_β and M_ζ are the generalized aerodynamic forces and the following definitions have been introduced:

$$\begin{aligned} p^2 &= 1 + \bar{\omega}_\beta^2 \\ \bar{\omega}_\beta^2 &= k_\beta/\Omega^2 I \\ \bar{\omega}_\zeta^2 &= k_\zeta/\Omega^2 I \end{aligned} \tag{14}$$

If a lag-flap hinge sequence is employed, the hub-fixed rotating axes xyz are related to the blade-fixed axes $x_2y_2z_2$ according to

$$\begin{Bmatrix} x \\ y \\ z \end{Bmatrix} = [T_{\rm LF}] \begin{Bmatrix} x_2 \\ y_2 \\ z_2 \end{Bmatrix} = [T_\zeta][T_\beta] \begin{Bmatrix} x_2 \\ y_2 \\ z_2 \end{Bmatrix} \tag{15}$$

Following the same steps as outlined above for the flap-lag hinge sequence leads to the same equations given as Eqs. (13a) and (13b). Hence, as far as the dynamic aspects are concerned, both hinge sequences yield the same second-degree equations. The generalized aerodynamic forces will be different in the two cases, however. These differences will become clear later.

Aerodynamics

The flow relative to the blade due to forward flight velocity V follows immediately from Fig. 2 as

$$V_a = \mu\Omega R\cos\psi\hat{e}_x - \mu\Omega R\sin\psi\hat{e}_y + \Omega R\lambda\hat{e}_z \tag{16}$$

This expression is independent of the hinge sequence. The total velocity relative to a blade mass element (aerodynamic + dynamic) is given by

$$V_{xyz} = V_a - \dot{\rho} \tag{17}$$

The total velocity for a flap-lag hinge sequence from Eq. 17 is

$$\begin{aligned} V_{xyz} = & [r(\cos\beta\sin\zeta\dot{\zeta} + \cos\zeta\sin\beta\dot{\beta} + \Omega\sin\zeta) \\ & + \mu\Omega R\cos\psi]\hat{e}_x - [r(\cos\zeta\dot{\zeta} + \Omega\cos\beta\cos\zeta) \\ & + \mu\Omega R\sin\psi]\hat{e}_y + [r(\sin\beta\sin\zeta\dot{\zeta} - \cos\zeta\cos\beta\dot{\beta}) + \Omega R\lambda]\hat{e}_z \end{aligned} \tag{18}$$

The total velocity expressed in the blade-fixed system $x_2y_2z_2$ is required in order to compute the aerodynamic forces acting on the blade. This is obtained from

$$V_{x_2y_2z_2} = [T_{\rm FL}]^T V_{xyz} \tag{19}$$

From Fig. 3, $V_{x_2y_2z_2}$ can also be expressed as

$$V_{x_2y_2z_2} = U_R\hat{e}_{x_2} - U_T\hat{e}_{y_2} - U_p\hat{e}_{z_2} \tag{20}$$

From Eqs. (18-20) the radial, tangential, and perpendicular components of the total velocity in blade-fixed axes for a flap-lag hinge sequence are

$$U_R = \mu\Omega R\cos\psi\cos\beta\cos\zeta - \mu\Omega R\sin\psi\sin\zeta + \Omega R\lambda\sin\beta\cos\zeta \tag{21a}$$

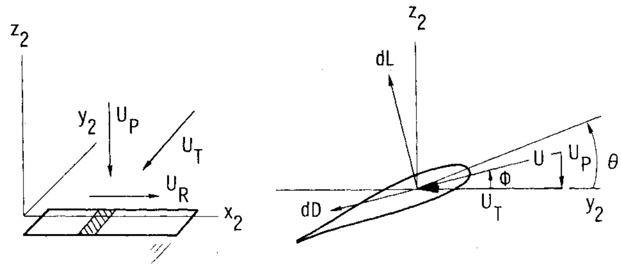

Fig. 3 Blade element velocities and forces.

$$U_T = r\dot{\zeta} + r\Omega\cos\beta + \mu\Omega R\cos\psi\cos\beta\sin\zeta$$
$$+ \mu\Omega R\sin\psi\cos\zeta + \underline{\Omega R\lambda\sin\beta\sin\zeta} \tag{21b}$$

$$U_P = r\dot{\beta}\cos\zeta + \underline{r\Omega\sin\beta\sin\zeta} + \mu\Omega R\cos\psi\sin\beta - \Omega R\lambda\cos\beta \tag{21c}$$

For a lag-flap hinge sequence, the expressions for U_R, U_T, and U_P are given by

$$U_R = \mu\Omega R\cos\psi\cos\beta\cos\zeta - \mu\Omega R\sin\psi\sin\zeta\cos\beta + \Omega R\lambda\sin\beta \tag{22a}$$

$$U_T = r\dot{\zeta}\cos\beta + r\Omega\cos\beta + \mu\Omega R\cos\psi\sin\zeta + \mu\Omega R\sin\psi\cos\zeta \tag{22b}$$

$$U_P = r\dot{\beta} + \mu\Omega R\cos\psi\sin\beta\cos\zeta - \Omega R\lambda\cos\beta - \underline{\mu\Omega R\sin\psi\sin\beta\sin\zeta} \tag{22c}$$

At this point, it is convenient to indicate and discuss differences which appear in the expressions for U_T and U_P as a consequence of the hinge sequence. Comparing the present U_T expressions through second degree, the only difference is the additional (underlined) term in Eq. (21b) for the flap-lag sequence. For the low inflows typical of helicopter rotors, however, that term is small compared to the remaining terms in that expression. Comparing the present U_P expressions, there are two differences. First, the underlined term in Eq. (21c) for the flap-lag sequence does not appear in the corresponding expression for the lag-flap sequence. This term will lead to aerodynamic pitch-lag and pitch-flap coupling terms associated with steady-state flapping and lagging in the linear perturbation equations in both hover and forward flight. The second difference in the U_P expressions is the presence of the underlined term in Eq. (22c) for the lag-flap sequence. This term will also lead to pitch-lag and pitch-flap coupling terms in forward flight. Hence, pitch-lag and pitch-flap coupling terms appear for both a flap-lag and lag-flap hinge sequence in the case of forward flight in contrast to the case of hover where these terms appear only for a flap-lag hinge sequence.

The lift and drag acting on an elemental section of the blade can be written directly as

$$\mathrm{d}L = \tfrac{1}{2}\rho acU^2\alpha\mathrm{d}r \tag{23a}$$

$$\mathrm{d}D = \tfrac{1}{2}\rho acU^2(C_{d_0}/a)\mathrm{d}r \tag{23b}$$

where (from Fig. 3)

$$\alpha = \theta - \phi = \theta - \tan^{-1}(U_P/U_T) \tag{24}$$

The section pitch angle θ, assuming no kinematic coupling and zero pretwist, is given by

$$\theta = \theta_c - \theta_{lc}\cos\psi - \theta_{ls}\sin\psi \tag{25}$$

Projecting $\mathrm{d}L$ and $\mathrm{d}D$ along y_2 and z_2 directions yields

$$\mathrm{d}F_{z_2} = \mathrm{d}L\cos\phi - \mathrm{d}D\sin\phi \tag{26a}$$

$$\mathrm{d}F_{y_2} = -\mathrm{d}L\sin\phi - \mathrm{d}D\cos\phi \tag{26b}$$

Combining Eqs. (23-26) leads to

$$\mathrm{d}F_{z_2} = \tfrac{1}{2}\rho ac\left[\alpha UU_T + \frac{C_{d_0}}{a}UU_P\right]\mathrm{d}r \tag{27a}$$

$$\mathrm{d}F_{y_2} = -\tfrac{1}{2}\rho ac\left[\alpha UU_P + \frac{C_{d_0}}{a}UU_T\right]\mathrm{d}r \tag{27b}$$

For the case of a flap-lag hinge sequence, the elemental forces in the hub-fixed rotating axes xyz follow from

$$\begin{Bmatrix} \mathrm{d}F_x \\ \mathrm{d}F_y \\ \mathrm{d}F_z \end{Bmatrix} = [T_{\mathrm{FL}}]\begin{Bmatrix} 0 \\ \mathrm{d}F_{y_2} \\ \mathrm{d}F_{z_2} \end{Bmatrix} \tag{28}$$

Using the principle of virtual work, the generalized aerodynamic forces are

$$M_\beta = \int_0^R \{\mathrm{d}F_{xyz}\}^T\left\{\frac{\partial\rho}{\partial\beta}\right\} = \int_0^R r\cos\zeta\mathrm{d}F_{z_2} \tag{29a}$$

$$M_\zeta = \int_0^R \{\mathrm{d}F_{xyz}\}^T\left\{\frac{\partial\rho}{\partial\zeta}\right\} = \int_0^R r\mathrm{d}F_{y_2} \tag{29b}$$

For a lag-flap hinge sequence the generalized aerodynamic forces are

$$M_\beta = \int_0^R r\mathrm{d}F_{z_2} \tag{30a}$$

$$M_\zeta = \int_0^R r\cos\beta\mathrm{d}F_{y_2} \tag{30b}$$

The induced flow v_i appearing in λ is calculated by equating the integrated thrust to the thrust from momentum theory and leads to the result

$$v_i = \frac{C_T\Omega R}{2\sqrt{\mu^2+\lambda^2}} \tag{31}$$

where

$$C_T = \frac{b}{2\pi}\frac{1}{\rho\pi\Omega^2R^4}\int_0^{2\pi}\int_0^R \mathrm{d}F_{z_0}\mathrm{d}\psi \tag{32}$$

Equations (13a) and (13b) in combination with Eqs. (31) and (32) comprise the full nonlinear flap-lag equations of motion for both the flap-lag and lag-flap hinge sequences using the appropriate definitions of M_β and M_ζ.

Linearization of Equations

Common practice in dealing with the nonlinear equations is to perturb them about some steady-state equilibrium condition by writing

$$\beta = \beta_0 + \Delta\beta \qquad \zeta = \zeta_0 + \Delta\zeta \tag{33}$$

where β_0 and ζ_0 are the steady-state values of β and ζ, and $\Delta\beta$ and $\Delta\zeta$ are the perturbations from equilibrium. Substituting Eqs. (33) into the nonlinear equations of motion leads to two sets of equations, one for the trim solution involving β_0 and

ζ_0 and another for the perturbation variables $\Delta\beta$ and $\Delta\zeta$. Linear perturbation equations are obtained by the usual practice of discarding all perturbation terms of second degree or higher.

Trim Equations

In the trim position, the rotor is maintained at a fixed value of thrust coefficient. Referring to Fig. 2, the requirement for horizontal and vertical force equilibrium leads to the following equations

$$D_P + H\cos\alpha + T\sin\alpha = 0 \tag{34a}$$

$$T\cos\alpha = mg \tag{34b}$$

where

$$H = \frac{b}{2\pi}\int_0^{2\pi}\int_0^R dF_{X_0}\,d\psi \tag{35a}$$

$$T = \frac{b}{2\pi}\int_0^{2\pi}\int_0^R dF_{z_0}\,d\psi \tag{35b}$$

$$dF_{X_0} = dF_{x_0}\cos\psi - dF_{y_0}\sin\psi \tag{35c}$$

and the elemental inplane forces dF_{x_0} and dF_{y_0} and normal force dF_{z_0} are the steady-state values obtained from Eq. 28. The rotor pitching and rolling-moment equilibrium at the trim condition is achieved with cyclic pitch sufficient to suppress first harmonic flapping. Since the steady-state cyclic flapping angles are zero there is no difference between the shaft angle and the rotor angle. For simplicity, it is assumed that the steady-state cyclic lagging angles are zero. This reduces by two the required number of trim equations. The flap and lag equations defining the trim conditions thus assume the form

$$p^2\beta_0 = \frac{1}{I\Omega^2}\int_0^R r\cos\zeta_0 dF_{z_{2_0}} \equiv M_{\beta_0}/I\Omega^2 \tag{36a}$$

$$\bar{\omega}_\zeta^2\zeta_0 = \frac{1}{I\Omega^2}\int_0^R r dF_{y_{2_0}} \equiv M_{\zeta_0}/I\Omega^2 \tag{36b}$$

The last equation required to complete the set of trim equations is

$$\mu\tan\alpha = \lambda + \frac{C_T/2}{\sqrt{\mu^2+\lambda^2}} \tag{37}$$

There are 11 equations in the nine unknowns β_0, ζ_0, θ_c, θ_{lc}, θ_{ls}, v_i, λ, H, and α. Two of the equations are redundant because the steady-state cyclic lag angles have been set to zero. The trim equations for a lag-flap hinge sequence can be obtained from the equations given above for the flap-lag sequence by simply substituting appropriate expressions for dF_{X_0} and dF_{z_0} in Eqs. (35a) and (35b) and for M_{β_0} and M_{ζ_0} in Eqs. (36a) and (36b). The trim equations are nonlinear in the trim parameters. However, with the exception of Eq. 31, only the linearized trim equations are considered in this paper. In this case, the trim equations are the same for both the flap-lag and lag-flap hinge sequences.

Perturbation Equations

The perturbation equations for flap-lag stability are obtained by substituting the expressions given by Eq. (33) into the full nonlinear equations and subtracting out the trim equations given in Eqs. (36a) and (36b). These manipulations ultimately lead to

$$\Delta\ddot\beta + 2\Omega\beta_0\Delta\dot\zeta + 2\zeta_\beta p\Omega\Delta\dot\beta + p^2\Omega^2\Delta\beta = \Delta M_\beta/I \tag{38a}$$

$$\Delta\ddot\zeta - 2\Omega\beta_0\Delta\dot\beta + 2\zeta_\zeta\bar\omega_\zeta\Omega\Delta\dot\zeta + \bar\omega_\zeta^2\Omega^2\Delta\zeta = \Delta M_\zeta/I \tag{38b}$$

where

$$\Delta M_\beta = \int_0^R [r\cos\zeta_0\Delta(dF_{z_2}) - r\zeta_0\Delta\zeta dF_{z_{2_0}}] \tag{39a}$$

$$\Delta M_\zeta = \int_0^R r\Delta(dF_{y_2}) \tag{39b}$$

for a flap-lag hinge sequence and

$$\Delta M_\beta = \int_0^R r\Delta(dF_{z_2}) \tag{40a}$$

$$\Delta M_\zeta = \int_0^R [r\cos\beta_0\Delta(dF_{y_2}) - r\beta_0\Delta\beta dF_{y_{2_0}}] \tag{40b}$$

for a lag-flap hinge sequence. Expanding $\Delta(dF_{z_2})$ and $\Delta(dF_{y_2})$ in Taylor series about the steady-state equilibrium condition leads to

$$\begin{aligned}\Delta(dF_{z_2}) &= \frac{\partial}{\partial U_P}(dF_{z_2})\Big|_0 \Delta U_P + \frac{\partial}{\partial U_T}(dF_{z_2})\Big|_0 \Delta U_T\\ &= ½\rho acdr\{-U_{T_0}\Delta U_P + [2U_{T_0}(\theta_c\\ &\quad -\theta_{lc}\cos\psi - \theta_{ls}\sin\psi) - U_{P_0}]\Delta U_T\}\end{aligned} \tag{41a}$$

$$\begin{aligned}\Delta(dF_{y_2}) &= \frac{\partial}{\partial U_P}(dF_{y_2})\Big|_0 \Delta U_P + \frac{\partial}{\partial U_T}(dF_{y_2})\Big|_0 \Delta U_T\\ &= -½\rho acdr\Big\{[U_{T_0}(\theta_c - \theta_{lc}\cos\psi - \theta_{ls}\sin\psi)\\ &\quad -2U_{P_0}]\Delta U_P + \Big[U_{P_0}(\theta_c - \theta_{lc}\cos\psi\\ &\quad -\theta_{ls}\sin\psi) + 2U_{T_0}\frac{C_{d_0}}{a}\Big]\Delta U_T\Big\}\end{aligned} \tag{41b}$$

While simplifying these expressions it has been assumed that $U_{P_0}/U_{T_0} \ll 1$ and $C_{d_0}/a \ll 1$. For a flap-lag hinge sequence

$$(U_{P_0})_{FL} = \Omega R(-\lambda + \mu\beta_0\cos\psi) + r\Omega\zeta_0\beta_0 \tag{42a}$$

$$\begin{aligned}(\Delta U_P)_{FL} &= r\Delta\dot\beta + r\Omega(\beta_0\Delta\zeta + \zeta_0\Delta\beta)\\ &\quad + \lambda\Omega R\beta_0\Delta\beta + \mu\Omega R\Delta\beta\cos\psi\end{aligned} \tag{42b}$$

$$(U_{T_0})_{FL} = r\Omega + \mu\Omega R(\sin\psi + \zeta_0\cos\psi) + \beta_0\zeta_0\Omega R\lambda \tag{42c}$$

$$\begin{aligned}(\Delta U_T)_{FL} &= r\Delta\dot\zeta - r\Omega\beta_0\Delta\beta + \lambda\Omega R(\beta_0\Delta\zeta + \zeta_0\Delta\beta)\\ &\quad + \mu\Omega R\Delta\zeta\cos\psi - \mu\Omega R\sin\psi\zeta_0\Delta\zeta - \mu\Omega R\cos\psi\beta_0\zeta_0\Delta\beta\end{aligned} \tag{42d}$$

For a lag-flap hinge sequence

$$(U_{P_0})_{LF} = (U_{P_0})_{FL} - r\Omega\zeta_0\beta_0 - \mu\Omega R\beta_0\zeta_0\sin\psi \tag{43a}$$

$$\begin{aligned}(\Delta U_P)_{LF} &= (\Delta U_P)_{FL} - r\Omega(\beta_0\Delta\zeta + \zeta_0\Delta\beta)\\ &\quad - \mu\Omega R\sin\psi(\beta_0\Delta\zeta + \zeta_0\Delta\beta) - \mu\Omega R\cos\psi\beta_0\zeta_0\Delta\zeta\end{aligned} \tag{43b}$$

$$(U_{T_0})_{LF} = (U_{T_0})_{FL} - \Omega R\lambda\beta_0\zeta_0 \tag{43c}$$

$$\begin{aligned}(\Delta U_T)_{LF} &= (\Delta U_T)_{FL} - \Omega R\lambda(\beta_0\Delta\zeta + \zeta_0\Delta\beta)\\ &\quad + \mu\Omega R\cos\psi\beta_0\zeta_0\Delta\beta\end{aligned} \tag{43d}$$

Numerical Results

Some numerical results which illustrate the effect of hinge sequence on blade flap-lag stability in hover are shown in Fig. 4. The solid curves are for a flap-lag hinge sequence and correspond to the case in which the lag hinge flaps with the blade; while the dashed curve is for a lag-flap hinge sequence and corresponds to the case in which the flap hinge lags with the blade. The value of θ_c indicated in the figure is the critical collective pitch angle above which the blade becomes unstable. Combinations of flapping frequencies p and lagging frequencies $\bar{\omega}_\zeta$ leading to an instability are given by the areas inside the boundaries. It is clear that the stability of the system is different depending on which hinge sequence is employed and that the magnitude of the difference depends on the particular combination of flap and lag frequencies which are selected. Three other conclusions follow from Fig. 4. First, for a blade having a lag-flap hinge sequence there is no instability for any lagging frequency $\bar{\omega}_\zeta$ if the flapping frequency $p=1$. This result is in agreement with the result given in Ref. 11. Second, for a flap-lag hinge sequence an instability is possible at $p=1$ for blades which are stiff inplane ($\bar{\omega}_\zeta > 1$). This is a new observation. Third, pitch-flap coupling associated with steady-state lagging has only a small effect on stability, at least for the particular rotor parameters indicated in Fig. 4.

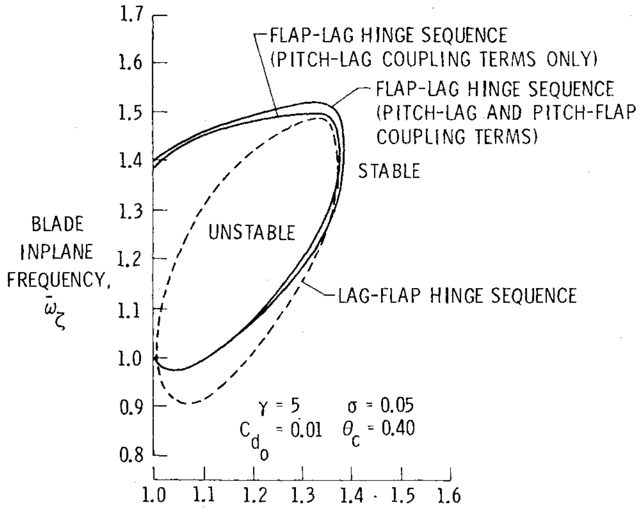

Fig. 4 Effect of hinge sequence on flap-lag stability in hover.

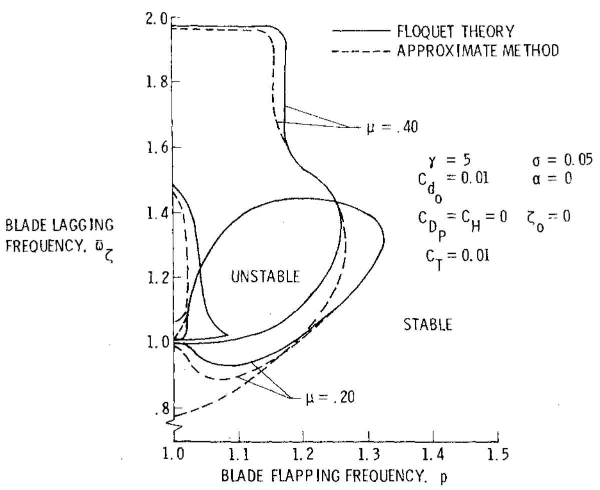

Fig. 5 Comparison of flap-lag stability boundaries obtained from Floquet theory and approximate method for lag-flap hinge sequence.

Some numerical results for the case of forward flight are presented in Figs. 5–7. Two different methods of solution were employed to obtain the forward flight results. The first method of solution is based on Floquet-Liapunov theory for solving linear differential equations with periodic coefficients and can be applied to the equations of motion expressed in either a rotating or a nonrotating system of coordinates. The second method of solution is based on solving an approximate system of linear equations with constant coefficients which is obtained by transforming the equations of motion with periodic coefficients to a nonrotating, space-fixed coordinate system and time averaging the periodic coefficients. Both of these methods of solution are discussed in Ref. 20.

The stability boundaries obtained using the constant coefficient approximation are compared with those obtained using Floquet theory in Fig. 5 for a blade having a lag-flap hinge sequence and operating at advance ratios of 0.20 and 0.40. The combination of flap and lag frequencies which lead to an instability are within the area enclosed by each of the boundaries. It should be noted that the blade is not stable for all values of $\bar{\omega}_\zeta$ at $p=1$ as in hover (see Fig. 4) since the region of instability now extends down to $p=1$ and includes a range of values of $\bar{\omega}_\zeta$ around $\bar{\omega}_\zeta = 1$. The instability in the vicinity of $\bar{\omega}_\zeta = 1$ is a parametric instability and is a consequence of the periodicity associated with forward flight. Such instabilities should be expected whenever $\bar{\omega}_\zeta$ is close to some integer multiple(s) of ½ per rev. The overall agreement between the results of the approximate method and Floquet theory for both $\mu = 0.20$ and $\mu = 0.40$ is good except in the vicinity of $\bar{\omega}_\zeta = 1$. In this region the Floquet results yield a very narrow region of parametric instability for both values of μ while the approximate method indicates that the region of parametric

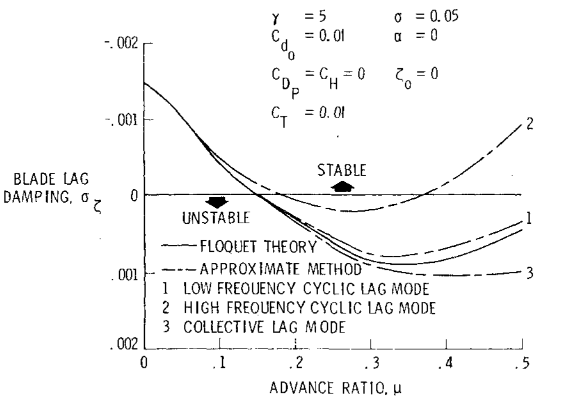

Fig. 6 Comparison of lag mode damping from Floquet theory and approximate method for lag-flap hinge sequence: $p = 1.15$, $\bar{\omega}_\zeta = 1.40$.

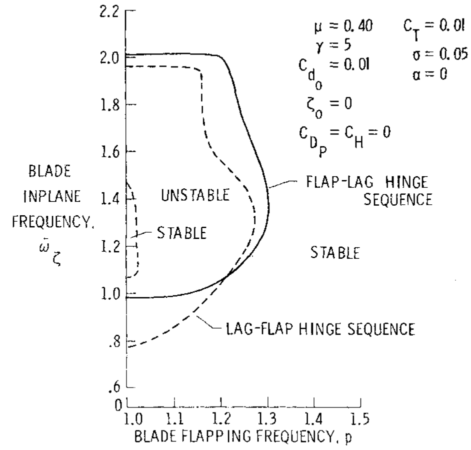

Fig. 7 Effect of hinge sequence on flap-lag stability in forward flight (approximate method; $\mu = 0.40$).

instability widens with increasing μ. It should be noted, however, that the behavior of the approximate solution with increasing μ is conservative from a stability point of view. The Floquet theory results shown in Fig. 5 are in good agreement with similar results obtained in Ref. 12 using Floquet theory except in the vicinity of $\bar{\omega}_\zeta = 1$, where Ref. 12 shows the blade to be free from parametric instability and stable for all $\bar{\omega}_\zeta$ at $p=1$. Figure 5 clearly demonstrates that the constant coefficient approximation is in excellent agreement with Floquet theory for $\mu=0.20$ and in generally good agreement for $\mu=0.40$. These findings are at variance with that of Ref. 12 which concluded that a constant coefficient approximation was good only for $\mu<0.10$. This indicates that the present approximate method, which is based on time averaging the periodic coefficients of the equations of motion expressed in the fixed system, is significantly better than a constant coefficient approximation which is obtained by time averaging in the rotating system, such as done in Ref. 12. Thus, the present results reconfirm the range of applicability of the constant coefficient approximation established in Ref. 20.

A comparison of the variation of lag mode damping with advance ratio predicted using Floquet theory and the approximate method for a lag-flap hinge sequence is made in Fig. 6.‡ The results obtained by applying Floquet theory to the equations with periodic coefficients expressed in both rotating and nonrotating coordinate systems are identical and hence the two curves are coincident, as should be expected. The damping in all three lag modes obtained by the approximate method agrees well with the damping predicted using Floquet theory at low advance ratios, where the influence of the periodic coefficients is small. As the advance ratio is increased, the damping associated with the low-frequency cyclic lag mode and the collective lag mode remain in good to fair agreement with the Floquet theory damping results through $\mu \simeq 0.50$. The damping associated with the high-frequency cyclic lag mode, although exhibiting the proper trend, is in poor numerical agreement with the damping obtained using Floquet theory. It should be noted, however, that the damping of the mode most critical from a stability point of view (mode #3) is in good agreement with Floquet theory through $\mu \simeq 0.40$. In particular, it should be noted that the advance ratio for the onset of instability predicted using the approximate method is in good agreement with that predicted using Floquet theory.

The influence of hinge sequence on stability in forward flight as predicted using the constant coefficient approximation is indicated in Fig. 7 for $\mu=0.40$. Again, the regions within the boundaries represent combinations of flap and lag frequencies which lead to an instability. As in the case of hover, the stability of the system in forward flight can be sensitive to the hinge sequence employed, depending on the system parameters.

The numerical results presented have all been based on the assumption that the blade has zero structural damping. In practice, a blade will have some inherent structural damping, albeit small. A cursory examination of the effect of blade lead-lag structural damping on stability showed that 0.5% of critical damping eliminated the regions of instability for the particular parameters considered in the numerical examples. However, additional studies on the influence of structural damping should be conducted over a broad range of practical system parameters in order to provide a more realistic assessment on the effect of damping.

Hover Stability Using Routh's Criterion

It is of interest to examine whether the main conclusions established earlier for the case of hover by a numerical analysis of the perturbation equations which retain all the linear terms can be established more simply using Routh's criterion applied to the characteristic equation associated with a simplified form of the perturbation equations which retain only the predominant linear terms. Specializing the equations of motion developed above to the case of hover and taking the Laplace transform assuming zero initial conditions, the resulting perturbation equations of motion corresponding to a flap-lag hinge sequence are given by

$$\begin{bmatrix} s^2+\frac{\gamma}{8}s+p^2+\frac{\gamma}{8}\left[\zeta_0(1+2A\theta_c-C)+2\beta_0(\theta_c-A)\right] & \left[2\beta_0-\frac{\gamma}{8}(2\theta_c-A)\right]s+\frac{\gamma}{8}\left[\beta_0(1+2A\theta_c-C)+\zeta_0(\theta_c-A)\right] \\ \left[\frac{\gamma}{8}(\theta_c-2A)-2\beta_0\right]s+\frac{\gamma}{8}\left[\zeta_0\left(\theta_c-2A-C\theta_c-2A\frac{C_{d_0}}{a}\right)-2\beta_0\left(A\theta_c+\frac{C_{d_0}}{a}-C\right)\right] & s^2+\frac{\gamma}{8}\left(2\frac{C_{d_0}}{a}+A\theta_c\right)s+\bar{\omega}_\zeta^2+\frac{\gamma}{8}\left[\beta_0(\theta_c-2A-C\theta_c)\right] \end{bmatrix}\begin{Bmatrix}\Delta\beta \\ \Delta\zeta\end{Bmatrix}=\{0\} \tag{44}$$

while those corresponding to a lag-flap hinge sequence are given by

$$\begin{bmatrix} s^2+\frac{\gamma}{8}s+p^2+\frac{\gamma}{8}\left[2\beta_0(\theta_c-A)\right] & \left[2\beta_0-\frac{\gamma}{8}(2\theta_c-A)\right]s \\ \left[\frac{\gamma}{8}(\theta_c-2A)-2\beta_0\right]s+\frac{\gamma}{8}\left[3\beta_0\left(C-A\theta_c-\frac{C_{d_0}}{a}\right)\right] & s^2+\frac{\gamma}{8}\left[2\frac{C_{d_0}}{a}+A\theta_c\right]s+\bar{\omega}_\zeta^2 \end{bmatrix}\begin{Bmatrix}\Delta\beta \\ \Delta\zeta\end{Bmatrix}=\{0\} \tag{45}$$

where s is the Laplace variable,

$$A=\frac{4}{\Omega R^4}\int_0^R r^2 v_i \mathrm{d}r \qquad C=\frac{4}{\Omega^2 R^4}\int_0^R r v_i^2 \mathrm{d}r \tag{46}$$

‡The Floquet results shown in Fig. 6 do not agree with the fixed system results shown in Ref. 20 because of two card punch errors in the computer program which were only recently identified. It should be noted that these errors did not affect the onset of instability predicted by Floquet theory in Ref. 20. In addition, the results obtained in both Refs. 1 and 20 using the constant coefficient approximation are not affected by these errors. Thus, the stability boundaries shown in Refs. 1 and 20, as well as the conclusions cited therein, remain unchanged.

and all terms containing the product $\beta_0\ \zeta_0$ have been discarded. Zero structural damping has also been assumed. By virtue of discarding the terms containing the product $\beta_0\ \zeta_0$, the steady-state equations defining β_0 and ζ_0 are independent of the hinge sequence and are given by

$$\begin{bmatrix} p^2 & 0 \\ 0 & \bar{\omega}_\zeta^2 \end{bmatrix} \begin{Bmatrix} \beta_0 \\ \zeta_0 \end{Bmatrix} = \frac{\gamma}{8} \begin{Bmatrix} \theta_c - A \\ -\left(A\theta_c + \dfrac{C_{d_0}}{a} - C\right) \end{Bmatrix} \tag{47}$$

Comparing Eqs. (44) and (45), it is clear that the perturbation equations developed for a lag-flap hinge sequence are not rigorously applicable to a blade which has a flap-lag hinge sequence.

It should be noted that all the aerodynamic terms involving β_0 and ζ_0 in Eq. (44) are stiffness terms. These aerodynamic stiffness terms are further simplified by introducing an ordering scheme to reduce the algebraic manipulations while applying Routh's criterion. In this simplification, it is first assumed that β_0, ζ_0, θ_c, and A are of first order and that C and C_{d_0}/a are of second order. Then, all aerodynamic stiffness terms of second order or higher are discarded in the flap equation and all aerodynamic stiffness terms of third order or higher are discarded in the lag equation. Under these conditions, the perturbation equations for a flap-lag hinge sequence given by Eq. (44) reduce to

$$\begin{bmatrix} s^2 + \frac{\gamma}{8} s + p^2 + \underline{\frac{\gamma}{8}\zeta_0} & \left[2\beta_0 - \frac{\gamma}{8}(2\theta_c - A)\right]s + \underline{\underline{\frac{\gamma}{8}\beta_0}} \\ \left[\frac{\gamma}{8}(\theta_c - 2A) - 2\beta_0\right]s + \underline{\frac{\gamma}{8}(\theta_c - 2A)\zeta_0} & s^2 + \frac{\gamma}{8}\left[2\frac{C_{d_0}}{a} + A\theta_c\right]s + \underline{\underline{\frac{\gamma}{8}(\theta_c - 2A)\beta_0}} + \bar{\omega}_\zeta^2 \end{bmatrix} \begin{Bmatrix} \Delta\beta \\ \Delta\zeta \end{Bmatrix} = \{0\} \tag{48}$$

It should be noted that the ordering scheme employed leads to the retention of the aerodynamic stiffness term $(\gamma/8)(\theta_c - 2A)\beta_0$ in the lag equation. This term may not be neglected compared to ω_ζ^2 for articulated rotor blades which have very low inplane frequencies. The simplified perturbation equations for a lag-flap hinge sequence which follow from Eq. (45) have the same form as Eq. (48) but without the underlined terms. The steady-state equations are unchanged and are still given by Eq. (47). The doubly underlined terms in Eqs. (48) are the pitch-lag coupling terms and the singly underlined terms are the pitch-flap coupling terms associated with steady-state values of β and ζ.

Applying Routh's criterion to the characteristic equation obtained from Eq. (48) after setting ζ_0 to zero for further simplicity, the requirement for stability is given by the expression

$$\begin{aligned}
&(A\theta_c + D)(W-P)^2 + \eta^2 WD(1 + A\theta_c + D) + \eta^2 DP(A\theta_c \\
&+ D)(1 + A\theta_c + D) - (PD + PA\theta_c + W)\beta_0{}^2[2(P \\
&- 1)(2-P)][1 + A\theta_c + D] + \underline{2\beta_0{}^2\{P + \eta^2 D(1 + A\theta_c} \\
&\underline{+ D + \eta\beta_0(\theta_c - 2A)(1 + A\theta_c + D) - \beta_0{}^2[2(P-1)(2} \\
&\underline{- P)](1 + A\theta_c + D) + W(A\theta_c + D) - 2\beta_0{}^2\} - \eta P\beta_0(\theta_c} \\
&\underline{- 2A)(1 + A\theta_c + D) + \eta W\beta_0(\theta_c - 2A)(1 + A\theta_c + D)} \\
&\underline{- 2P\beta_0{}^2(A\theta_c + D) - 2W\beta_0{}^2} > 0
\end{aligned} \tag{49}$$

where

$$D = 2C_{d_0}/a, \qquad P = p^2, \qquad W = \bar{\omega}_\zeta^2, \qquad \eta = \gamma/8 \tag{50}$$

The pitch-lag coupling terms which are associated with a flap-lag hinge sequence are underlined in Eq. (49). Several conclusions follow from Eq. (49). First, for $P = p^2 = 1$ and no additional terms there is no possibility of instability for any $\bar{\omega}_\zeta$, which is in agreement with the numerical results of Fig. 4 and the results of Ref. 11. Second, making assumptions similar to those in Ref. 3 ($p = 1$, $\theta_c = \beta_0$, $A = 0$) and including the underlined terms Eq. (49) reduces to

$$2\frac{C_{d_0}}{a}(\bar{\omega}_\zeta^2 - 1)^2 + \bar{\omega}_\zeta^2 2\frac{C_{d_0}}{a} + \underline{\beta_0^2(1 - \bar{\omega}_\zeta^2)} > 0 \tag{51}$$

where several third and higher order terms associated with drag and β_0 have been discarded. It is clear from Eq. (51) that for soft-inplane ($\bar{\omega}_\zeta \ll 1$) rotors there is no possibility for instability. This result is in agreement with Ref. 3 as well as the numerical results of Fig. 4. Third, for a stiff-inplane $\bar{\omega}_\zeta > 1$) rotor, Eq. (51) indicates that instability is possible. This result is also in agreement with the numerical results of Fig. 4. The possibility of an instability for $\bar{\omega}_\zeta > 1$ is a direct consequence of the underlined terms in Eq. (51), which, in turn, are associated with the inclusion of the pitch-lag coupling terms in Eq. (48). As pointed out earlier, the possibility of an instability at $p = 1$ for a blade in which the lag hinge flaps is a new result. Thus, all the conclusions established using Routh's criterion applied to the characteristic equation associated with a simplified form of the perturbation equations which retain only the predominant linear terms are in agreement with the numerical results established earlier using the perturbation equations which retain all the linear terms.

Conclusions

The principal findings of the present study may be summarized as follows:

1) Several differences in the equations of motion for blade flap-lag stability in the existing literature have been identified. A rigorous and systematic development of these equations for a rigid articulated blade in both hover and forward flight yields some *linear* coupling terms associated with blade steady-state flapping and lagging in the perturbation equations for the case in which the lag hinge flaps with the blade. The effect of these differences on stability have not been clearly addressed in the literature.

2) For a rigid hinged blade or a hingeless blade treated by virtual hinges, the appearance of these coupling terms in the equations of motion depends on whether or not the lag hinge flaps with the blade. For the particular case in which the lag hinge flaps with the blade, a flap-lag instability was shown to be possible for an articulated blade without hinge offset ($p = 1$) and no structural damping. This is a new observation.

3) The pitch-lag coupling terms associated with a flap-lag hinge sequence have varying degrees of influence on flap-lag stability in both hover and forward flight, depending on the system parameters. Pitch-flap coupling associated with

steady-state lagging was found to have only a small effect on stability for the range of parameters investigated.

4) The applicability of an approximate method of analysis based on time averaging the periodic coefficients of the flap-lag equations of motion expressed in the fixed system was demonstrated up to $\mu < 0.40$.

References

[1]Kaza, K.R.V. and Kvaternik, R.G., "A Critical Examination of the Flap-Lag Dynamics of Helicopter Rotor Blades in Hover and in Forward Flight," presented at the 32nd Annual National V/STOL Forum of the American Helicopter Society, Washington, D.C., May 1976.

[2]Morduchow, M. and Hinchey, F.G., "Theoretical Analysis of Oscillations in Hovering of Helicopter Blades with Inclined and Offset Flapping and Lagging Hinge Axes," NACA TN 2226, Dec. 1950.

[3]Chou, P.C., "Pitch-Lag Instability of Helicopter Rotors," *Journal of the American Helicopter Society*, Vol. 3, July 1958, pp. 30-39.

[4]Blake, B.B., Burkam, J.E., and Loewy, R.G., "Recent Studies of the Pitch-Lag Instabilities of Articulated Rotors," *Journal of the American Helicopter Society*, Vol. 6, 1961, pp. 13-21.

[5]Hohenemser, K.H. and Heaton, P.W., Jr., "Aeroelastic Instability of Torsionally-Rigid Helicopter Blades," *Journal of the American Helicopter Society*, Vol. 12(2), April 1967, pp. 1-13.

[6]Jenkins, J.L., Jr., "A Numerical Method for Studying the Transient Blade Motions of a Rotor With Flapping and Lead-Lag Degrees of Freedom," NASA TN D-4195, Oct. 1967.

[7]Gaffey, T.M., "The Effect of Positive Pitch-Flap Coupling (Negative δ_3) on Rotor Blade Motion Stability and Flapping," *Journal of the American Helicopter Society*, Vol. 14(2), April 1969, pp. 49-67.

[8]Johnson, R.L. and Hohenemser, K.H., "On the Dynamics of Lifting Rotors With Thrust or Tilting Moment Feedback Controls," *Journal of the American Helicopter Society*, Vol. 15(1), Jan. 1970, pp. 42-54.

[9]Hall, W.E., Jr., "Application of Floquet Theory to the Analysis of Rotory-Wing VTOL Stability," SUDAAR Report 400, Stanford University, Feb. 1970.

[10]Tong, P., "The Nonlinear Instability in Flap-Lag of Rotor Blades in Forward Flight," NASA CR-114524, Oct. 1971.

[11]Ormiston, R.A. and Hodges, D.H., "Linear Flap-Lag Dynamics of Hingeless Helicopter Rotor Blades in Hover," *Journal of the Americal Helicopter Society*, Vol. 17(2), April 1972, pp. 2-14.

[12]Peters, D.A., "Flap-Lag Stability of Helicopter Rotor Blades in Forward Flight," *Journal of the Americal Helicopter Society*, Vol. 20(4), Oct. 1975, pp. 2-13.

[13]Friedmann, P. and Tong, P., "Dynamic Nonlinear Elastic Stability of Helicopter Rotor Blades in Hover and Forward Flight," NASA CR-114485, May 1972.

[14]Hodges, D.H. and Ormiston, R.A., "Stability of Elastic Bending and Torsion of Uniform Cantilevered Rotor Blades in Hover," Paper No. 73-405, AIAA/ASME/SAE 14th Structures, Structural Dynamics, and Materials Conference, Williamsburg, Va., March 1973.

[15]Hodges, D.H. and Ormiston, R.A., "Nonlinear Equations for Bending of Rotating Beams With Application to Linear Flap-Lag Stability of Hingeless Rotors," NASA TM X-2770, May 1973.

[16]Peters, D.A. and Ormiston, R.A., "The Effects of Second-Order Blade Bending on the Angle of Attack of Hingeless Rotor Blades," *Journal of the American Helicopter Society*, Vol. 18(4), Oct. 1973, pp. 45-48.

[17]Friedmann, P. and Silverthorn, L.J., "Aeroelastic Stability of Coupled Flap-Lag Motion of Hingeless Helicopter Blades at Arbitrary Advance Ratio," NASA CR-132431, Feb. 1974.

[18]Hodges, D.H. and Dowell, E.H., "Nonlinear Equations of Motion for the Elastic Bending and Torsion of Twisted Nonuniform Rotor Blades," NASA TN D-7818, Dec. 1974.

[19]Friedmann, P. and Shamie, J., "Aeroelastic Stability of Trimmed Helicopter Blades in Forward Flight," paper presented at the First European Rotorcraft and Powered Lift Aircraft Forum," University of Southampton, Southampton, England, Sept. 22-24, 1975.

[20]Kaza, K.R.V. and Hammond, C.E., "An Investigation of Flap-Lag Stability of Wind-Turbine Rotors in the Presence of Velocity Gradients and Helicopter Rotors in Forward Flight," presented at the AIAA/ASME/SAE 17th Structures, Structural Dynamics, and Materials Conference, Valley Forge, Pa., May 1976.